Correlation effects in the ground-state charge density of Mott insulating NiO: A comparison of *ab initio* calculations and high-energy electron diffraction measurements

S. L. Dudarev*
Max-Planck-Institut für Festkörperforschung, Heisenbergstraße 1, D-70569 Stuttgart, Germany

L.-M. Peng†
Department of Electronics, Peking University, Beijing 100871, China

S. Y. Savrasov
Max-Planck-Institut für Festkörperforschung, Heisenbergstraße 1, D-70569 Stuttgart, Germany

J.-M. Zuo
Department of Physics and Astronomy, Arizona State University, Tempe, Arizona 85287
(Received 7 June 1999)

Accurate high-energy electron diffraction measurements of structure factors of NiO have been carried out to investigate how strong correlations in the Ni $3d$ shell affect electron charge density in the *interior* area of nickel ions and whether the *ab initio* approaches to the electronic structure of strongly correlated metal oxides are in accord with experimental observations. The generalized gradient approximation and the local spin density approximation corrected by the Hubbard U term are found to provide the closest match to experimental measurements. The comparison of calculated and observed electron charge densities shows that correlations in the Ni $3d$ shell suppress covalent bonding between the oxygen and nickel sublattices.

Recent years have witnessed the largely unexpected[1] progress in the development of computational approaches to the evaluation of fundamental properties of materials from the first principles. The stimulus for this development was provided by the Hohenberg-Kohn theorem,[2] which establishes that the energy of the ground state of a solid is a functional of its one-electron density $\rho(\mathbf{r})$. The problem of accurate determination of $\rho(\mathbf{r})$ therefore acquires fundamental significance for the physics of materials *both* from the experimental *and* theoretical points of view. In cases where accurate experimentally measured and calculated charge densities are available (like, e.g., in the case of silicon[3]), the quality of *ab initio* approximations can be assessed on the basis of the agreement between experimental and theoretical data.

The Kohn-Sham method,[4] which provides a convenient way of carrying out density-functional calculations, in certain cases encounters serious difficulties. For example, it predicts metallic ground states for a number of late transition metal monoxides where metal ions have partly filled electronic shells. Nickel and cobalt monoxides are often quoted[5] as typical examples illustrating the failure of conventional density-functional methods to describe the effective one-particle band structure of Mott insulating materials.[6,7] Several modified density-functional schemes have been proposed lately to explain the nature of large band gaps observed for CoO and NiO. These schemes include the orbital polarization correction,[8] the self-interaction correction[9] and the local spin density approximation also taking into account the Hubbard U term (LSDA+U).[10,11] The approximations improve the description of the effective one-particle band structure of Mott insulators, and their validity is further confirmed by the recent studies of orbital ordering in transition metal compounds, see, e.g., Ref. 12.

At the same time it is widely appreciated that the new ''improved'' computational schemes represent a departure from the original formulation of density-functional theory.[2] The approximations employ functionals that depend not only on the spin density of electrons $\rho_\sigma(\mathbf{r})$ but also on the *orbital* occupation numbers that in turn depend on the choice of the basis functions. Calculations performed using the *ab initio* schemes result in better values for bandgaps and magnetic moments.[10] At the same time the modified energy functionals alter the relative occupancies of d states[13] and change the predicted distribution of charge density in the unit cell. This raises the question of how well the functionals describe the main entity of density-functional theory, namely, $\rho(\mathbf{r})$ itself.

In this paper, we investigate this issue by comparing the calculated and experimentally observed charge density distributions. We compare the structure factors of NiO that were measured using a recently developed highly accurate electron diffraction technique[14–16] and calculated theoretically using several *ab initio* linear muffin-tin orbital (LMTO)-based methods,[17,18] including the LSDA+U approach.

At present, there is no sufficiently accurate experimental information on the distribution of electron charge density in the unit cell of NiO or other similar transition metal oxides. The powder x-ray diffraction techniques that were successfully used to determine the equilibrium positions of ions in a unit cell,[19,20] do not have the accuracy required for observing the relatively small changes in the charge density resulting from the competition between covalent bonding and correlation effects. The convergent beam electron diffraction (CBED) technique used here takes advantage of the fact that electron beam can be focused on a small nearly perfect area of the sample and the resulting diffraction pattern can be simulated using highly accurate multiple scattering dynamical diffraction approach[15] therefore eliminating the extinction problem that limits the accuracy of x-ray techniques.

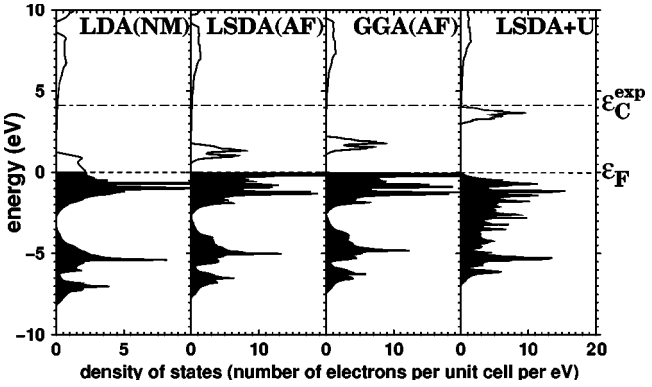

FIG. 1. The total density of states plots of NiO calculated assuming (a) a non-magnetic ground state and the local-density approximation (b) the type II AF ground state and the local spin density approximation (c) the type II AF ground state and the generalized gradient approximation (d) the type II AF ground state and the local spin density approximation corrected by the Hubbard U term (LSDA+U). ϵ_F denotes the Fermi energy and ϵ_C^{exp} shows the experimentally observed position of the bottom of the conduction band.

The high precision of electron diffraction measurements has made it possible to study subtle details of the charge density distribution in band insulators like MgO (Ref. 16) and Cu_2O.[21] In this paper we for the first time investigate how the interplay between covalent bonding and the Coulomb on-site repulsion between d electrons in a partially filled shell influences the charge density distribution in a crystal unit cell of a Mott insulating oxide.

Nickel monoxide is probably the most extensively studied Mott insulating material[22,23] and it is often referred to as the prototype of the entire class of ''anomalous'' transition-metal oxides. Depending on the type of approximation used in an *ab initio* calculation, the ground state of NiO is predicted to be a metal (LDA, nonmagnetic state), a $\sim$0.4 eV band-gap Mott insulator (LSDA, antiferromagnetic state), a $\sim$1.0 eV band-gap Mott insulator [generalized gradient approximation (GGA), antiferromagnetic state] or a $\sim$3.0 eV band-gap charge-transfer insulator (LSDA+U, antiferromagnetic state).

Figure 1 shows plots of the density of states calculated for the above four cases. The x-ray photoelectron spectroscopy data[23] agree best with the LSDA+U one-particle band structure[10,24] that shows that NiO is a charge-transfer insulator where the band gap separates filled oxygen $2p$ and empty nickel $3d$ states. The band structures of NiO calculated using either LSDA or GGA show instead that the band gap separates filled and empty nickel $3d$ states and that NiO is therefore a Mott-Hubbard insulator. In Fig. 1, we do not show the *projected* densities of states since they are similar to those shown in Ref. 7 for the LSDA case and in Ref. 24 for the LSDA+U case.

To characterize the distribution of electron charge density in a unit cell of NiO, we measured seven low-order energy dependent structure factors[25] $U(\mathbf{G})$ that are defined by

$$U(\mathbf{G})=\frac{2me^2}{\pi\hbar^2G^2\Omega}\left\{\int_\Omega \rho^{(T)}(\mathbf{r})\exp(-i\mathbf{G}\cdot\mathbf{r})d^3r - \sum_\alpha Z_\alpha \exp(-i\mathbf{G}\cdot\mathbf{r}_\alpha)\exp\left[-\frac{1}{2}\langle(\mathbf{G}\cdot\mathbf{u}_\alpha)^2\rangle\right]\right\}, \quad (1)$$

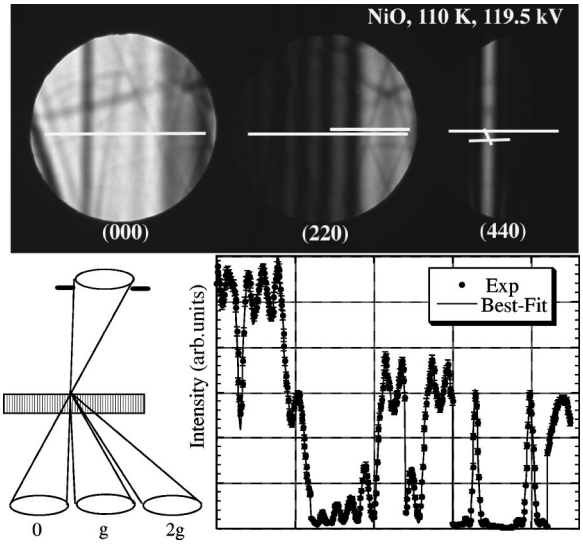

FIG. 2. An example of NiO structural factor measurement using convergent beam electron diffraction (CBED). The top is the experimentally recorded diffraction pattern with (220) and (440) strongly diffracted beams. The structural factors of (220) and (440) were obtained by fitting intensities along the indicated lines. The best fit is shown in bottom right. The schematic diagram on bottom-left shows the formation of CBED by focusing the electron beam on the top of a crystalline specimen.

where $\mathbf{G}$ is a reciprocal lattice vector, m is the relativistic electron mass, and Ω is the volume of the unit cell. Summation over α is performed over ions in a unit cell, Z_α is the charge, $\mathbf{r}_\alpha$ is the equilibrium position and $\mathbf{u}_\alpha$ is the thermal displacement of the respective nucleus. $\rho^{(T)}(\mathbf{r})$ is the electron density averaged over the thermal ensemble.

The experiment was performed using the LEO-912 Ω energy-filtering electron microscope with the Gatan liquid nitrogen cooled sample holder. The specimen used is a single crystal NiO cooled to about 110 K. The small rhombohedral distortion of NiO at 110 K was measured using higher-order Laue zone lines[26,27] to be $a=4.18$ Å and $\alpha=90.044°$. This small distortion was neglected in the charge-density study. The experimental CBED patterns were recorded using a 15-eV energy-filtering slit that was placed around the zero-loss peak. This was done to remove the contribution from inelastically scattered electrons that form continuous background due to plasmon and higher energy loss processes. Off-zone-axis systematic diffraction conditions were used to collect diffraction intensities for low-order reflections up to (440). The experimental patterns recorded using a slow-scan charge coupled device (CCD) camera were processed for the subsequent fitting using procedures described in Ref. 15. The refined values of the structure factors were obtained using the EXTAL program[15]. Figure 2 illustrates the level of agreement between the measured intensity variations and multiple-scattering dynamical diffraction simulations used in the refinement procedure. The error in the measured structure factors was estimated by comparing the results obtained using line scans taken at different positions (see Fig. 2).

The calculated values of structure factors (1) were obtained by integrating the self-consistent solutions $\rho(\mathbf{r})$ of the Kohn-Sham equations found using the LMTO method[17] and various approximations for the exchange-correlation poten-

TABLE I. The observed and calculated values of structure factors for NiO. The Debye-Waller temperature factors $B_{Ni}=8\pi^2\langle u_{Ni}^2\rangle$ and $B_O=8\pi^2\langle u_O^2\rangle$ for each calculated set were introduced following the procedure described in the text. The energy of the incident electrons equals $E_0=119.5$ keV. All the values listed in the table are given with the opposite sign and in Å^2 units (see Ref. 15). The *R*-factor is defined as $R=\Sigma_{\mathbf{G}}W_{\mathbf{G}}|U^{\rm th}(\mathbf{G})-U^{\rm exp}(\mathbf{G})|/|U^{\rm exp}(\mathbf{G})|$, where $U^{\rm th}(\mathbf{G})$ are the calculated and $U^{\rm exp}(\mathbf{G})$ are the experimentally measured values. The weight factors $W_{\mathbf{G}}$ are given by $W_{\mathbf{G}}=\sigma_{\mathbf{G}}^{-1}/(\Sigma_{\mathbf{G}}\sigma_{\mathbf{G}}^{-1})$ where $\sigma_{\mathbf{G}}$ represent experimental uncertainties. The error-bar of the *R* factor, δR, is given by $(\delta R)^2=\Sigma_{\mathbf{G}}W_{\mathbf{G}}\sigma_{\mathbf{G}}^2/|U^{\rm exp}(\mathbf{G})|^2$. Abbreviations NM and AF refer to nonmagnetic and antiferromagnetic states, respectively.

hkl	Observed values (std. dev. $\sigma_{\mathbf{G}}$)	ATOMS	LSDA (NM)	LSDA (AF)	LSDA+U (AF)	GGA (AF)	GGA+U (AF)
B_{Ni} (Å^2)	0.135 [a]	0.131	0.129	0.131	0.136	0.133	0.137
B_O (Å^2)	0.238 [a]	0.237	0.235	0.239	0.247	0.244	0.251
$-U(111)$	4.632×10^{-2} ($\pm0.012\times10^{-2}$)	4.401×10^{-2}	4.555×10^{-2}	4.597×10^{-2}	4.668×10^{-2}	4.642×10^{-2}	4.708×10^{-2}
$-U(200)$	9.083×10^{-2} ($\pm0.022\times10^{-2}$)	9.486×10^{-2}	9.187×10^{-2}	9.204×10^{-2}	9.181×10^{-2}	9.173×10^{-2}	9.151×10^{-2}
$-U(220)$	6.640×10^{-2} ($\pm0.036\times10^{-2}$)	6.756×10^{-2}	6.709×10^{-2}	6.716×10^{-2}	6.705×10^{-2}	6.703×10^{-2}	6.694×10^{-2}
$-U(311)$	2.482×10^{-2} ($\pm0.010\times10^{-2}$)	2.482×10^{-2}	2.482×10^{-2}	2.482×10^{-2}	2.481×10^{-2}	2.481×10^{-2}	2.481×10^{-2}
$-U(222)$	5.187×10^{-2} ($\pm0.026\times10^{-2}$)	5.336×10^{-2}	5.325×10^{-2}	5.318×10^{-2}	5.307×10^{-2}	5.311×10^{-2}	5.302×10^{-2}
$-U(400)$	4.456×10^{-2} ($\pm0.018\times10^{-2}$)	4.427×10^{-2}	4.455×10^{-2}	4.456×10^{-2}	4.457×10^{-2}	4.456×10^{-2}	4.457×10^{-2}
$-U(440)$	2.614×10^{-2} ($\pm0.034\times10^{-2}$)	2.613×10^{-2}	2.613×10^{-2}	2.611×10^{-2}	2.603×10^{-2}	2.610×10^{-2}	2.603×10^{-2}
R, δR	0.0045 [b], 0.0018	0.0215	0.0085	0.0067	0.0064	0.0049	0.0078

[a]Values calculated using the shell model (see text).

[b]R-factor evaluated on the basis of experimental uncertainties $\sigma_{\mathbf{G}}$.

tial. Calculations were performed assuming that the lattice constant was equal to $a=4.18$ Å (experimentally measured value) and using three κ-panels and 512 k points in the Brillouin zone. Convergence of the calculated values of structure factors was ensured by varying the number of k points and by introducing additional approximations (e.g., by taking into account the spin-orbit coupling). The exchange-correlation functionals were taken from[28] (LSDA),[29] (GGA) and[30] (LSDA+U). The values of $\overline{U}=6.2$ eV and $\overline{J}=0.95$ eV used in the LSDA+U calculation were determined from the analysis of electron energy-loss spectra and total energy calculations.[30]

The full self-consistent charge density was represented by a sum of two terms[18] where the first term $\tilde{\rho}(\mathbf{r})$ approximates the density in the region between the muffin-tin spheres and is continuous across the boundaries of the spheres. The second term approximates the density inside the muffin-tin spheres and is represented by a spherical harmonics expansion $Y_{lm}(\theta,\phi)$. Substituting this in Eq. (1) we arrive at

$$\int_\Omega \rho^{(T)}(\mathbf{r})\exp(-i\mathbf{G}\cdot\mathbf{r})d^3r = \exp\left[-\frac{1}{2}\langle(\mathbf{G}\cdot\mathbf{u})^2\rangle\right]\int_{\rm int.}\tilde{\rho}(\mathbf{r})\exp(-i\mathbf{G}\cdot\mathbf{r})d^3r + 4\pi\sum_\alpha \exp(-i\mathbf{G}\cdot\mathbf{r}_\alpha)\exp\left[-\frac{1}{2}\langle(\mathbf{G}\cdot\mathbf{u}_\alpha)^2\rangle\right] \times\sum_{l,m} Y_{lm}(\theta_{\mathbf{G}},\phi_{\mathbf{G}})\int \rho_{lm}^{(\alpha)}(r)j_l(Gr)r^2dr, \quad (2)$$

where $j_l(Gr)$ is a Bessel function, and $\mathbf{u}$ denotes the effective amplitude of thermal vibrations characterizing the motion of electrons in the interstitial region. No other thermal effects are taken into account in Eq. (2) in accord with spectroscopical data[31] showing no detectable changes in the electronic structure of NiO occurring in the temperature range between 0 °K and 615 °K.

A meaningful comparison between experiment and theory requires taking into account thermal vibrations of atomic nuclei. For example, the value of the (111) structure factor calculated in the LSDA(AF) approximation assuming that nuclei are frozen in their equilibrium positions equals -4.488×10^{-2} Å^2 to be compared with -4.597×10^{-2} Å^2 that was obtained assuming that $B_{Ni}=0.131$ Å^2 and $B_O=0.239$ Å^2. It is interesting that the calculated values of structure factors have proved to be almost insensitive to the choice of muffin-tin sphere radii. For example, we found that the above value of -4.597×10^{-2} Å^2 calculated assuming $R_{Ni}^{(MT)}=1.084$ Å and $R_O^{(MT)}=0.989$ Å changed by only $\sim0.1\%$ to -4.603×10^{-2} Å^2 when significantly smaller radii of muffin-tin spheres $R_{Ni}^{(MT)}=1.005$ Å and $R_O^{(MT)}=0.899$ Å were used in a calculation.

The difference between the values calculated for ''frozen'' and ''vibrating'' crystal lattices is approximately ten times the experimental uncertainty in the determination of this structure factor (see Table I) and this illustrates the significance of taking thermal vibrations into account. However, no reliable independent x-ray or neutron diffraction measurements on the Debye-Waller factors of Ni and O ions is available in the literature (notably, *negative* values of B_{Ni} were reported in a recent publication[20]). To provide a starting approximation for a subsequent refined search, we calculated the temperature factors of Ni and O using the shell model.

The shell model used for the theoretical evaluation of the Debye-Waller factors was developed by the Chalk River

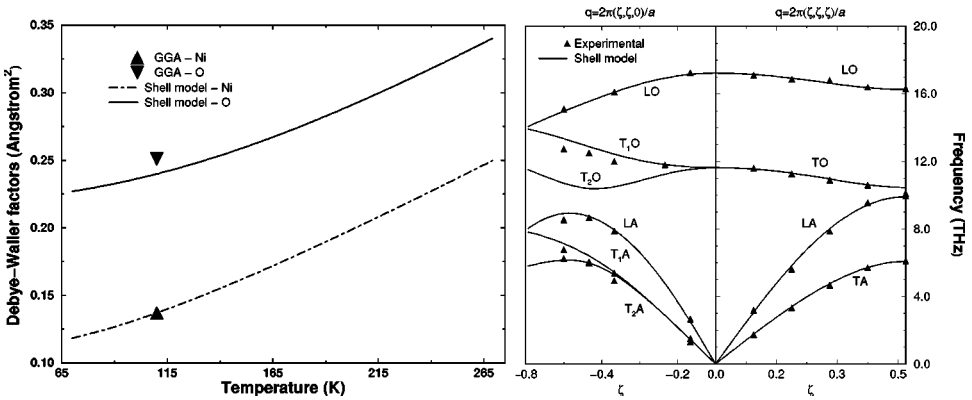

FIG. 3. Plots illustrating the fitting of the phonon dispersion curves along ⟨111⟩ and ⟨110⟩ directions, and the comparison between the values of the Debye-Waller factors evaluated using the shell model and found by comparing the experimentally measured and calculated structure factors.

group.[32] In this model an ion is represented by a massive core and a rigid shell describing valence electrons. Nine parameters in total were introduced to describe the lattice dynamics of NiO, these include the shell charges, force constants for springs connecting the cores and the shells as well as the first nearest neighbors (for the Ni^{2+} ions) and up to the second nearest neighbors (for the O^{2-} ions). The model parameters were obtained by fitting the calculated phonon dispersion curves to the experimentally measured ones.[33] For the chosen set of parameters of the model, we calculated the average thermal displacements $\langle \mathbf{u}^2 \rangle$ for all the modes of lattice vibrations, and also the Debye-Waller factors for both the nickel and oxygen ions. Figure 3 shows the fitted phonon dispersion curves plotted for the ⟨111⟩ and ⟨110⟩ directions, and also the temperature dependent Debye-Waller factors. We have also investigated several other implementations of the shell model but found that they led to no significant improvement in the description of the phonon dispersion curves.[34]

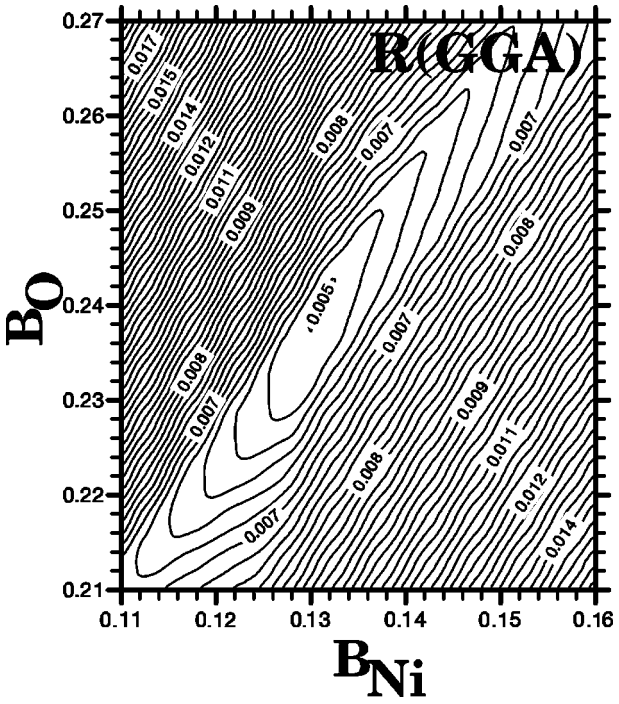

FIG. 4. A map showing the dependence of the R-factor on the two Debye-Waller factors B_{Ni} and B_O characterizing the amplitude of thermal vibrations of Ni and O ions in NiO. Values $B_{Ni} = 0.133$ Å^2 and $B_O = 0.244$ Å^2 correspond to the minimum of $R = 0.0049$.

To find more accurate values of the Debye-Waller parameters for each choice of the exchange-correlation potential used for *ab initio* calculations we plotted two-dimensional maps of the reliability factor R treating B_{Ni} and B_O as independent variables. (See Fig. 4.)

The values of B_{Ni} and B_O corresponding to the minimum of the R factor were then used to obtain the values of $U(\mathbf{G})$ shown in Table I. Results listed in Table I show that the estimated values of B_{Ni} and B_O are nearly independent on the choice of approximation used in *ab initio* calculations and that the spread of values of the Debye-Waller factor does not exceed 6%. The value of the Debye-Waller factor characterizing the thermal motion of electrons in the interstitial region was evaluated using two different approximations, namely, $\langle B \rangle = (B_O + B_{Ni})/2$ or $\langle B \rangle = (M_O B_O + M_{Ni} B_{Ni})/(M_O + M_{Ni})$. The difference between structure factors evaluated using these two approximations was found to be significantly smaller than the uncertainty of experimentally measured values of structure factors.

Apart from values calculated using the superposition of atomic densities, all the *ab initio* methods exhibit high (better than 1%) degree of accord with experimental data, with the exception of (111) and (222) structure factors. There is a large spread among theoretical values of the (111) structure factor, and the magnitude of this structure factor increases significantly with the inclusion of U. The (111) structure factor is most sensitive to the changes in the distribution of the density of valence electrons, and the differences among the theoretical models shows primarily the differences in the calculated ground state valence charge density. In terms of the overall R factor, the closest approximation to the experiment is provided by the generalized gradient approximation and by the LSDA+U approach (see Table I). Better agreement with the experimental value of the (111) structure factor is achieved with the GGA.

The difference between the GGA and the LSDA+U charge density distributions is illustrated in Fig. 5 where we mapped the densities calculated using the GGA and the LSDA+U approximations, subtracting from each of them the density corresponding to the nonmagnetic local-density approximation (LDA) solution.

Figure 5 shows that the symmetry of the deformation of electron density resulting from correlation effects remains the same both in LSDA+U and in GGA. At the same time there are significant differences in the radial structure of the density distributions around Ni ions calculated for the two cases. The LSDA+U approximation treats the wave func-

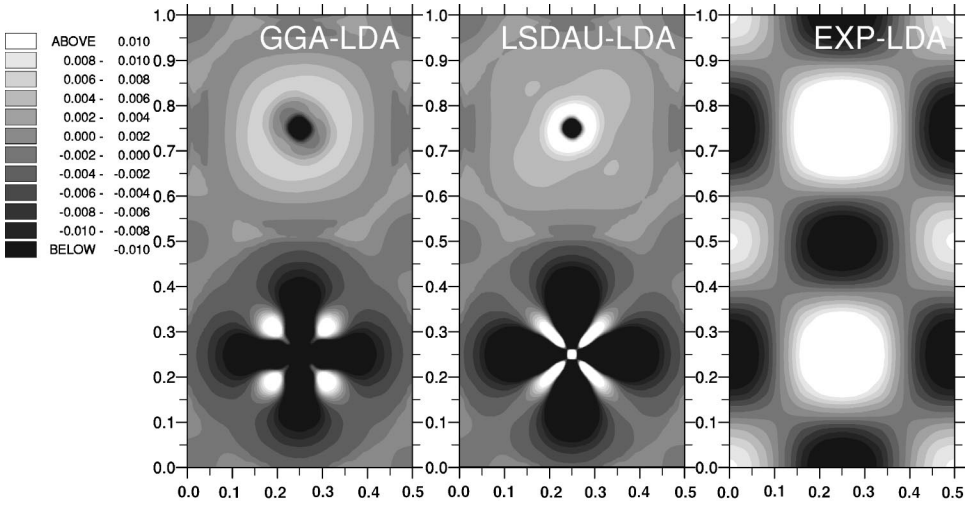

FIG. 5. Cross sections of charge-density distribution in the (100) plane of NiO calculated using the GGA and LSDA+U approximations. The two contour maps on the left-hand side show the difference between the self-consistent density distributions and the density calculated using the local density approximation for a nonmagnetic ground state. The map on the right-hand side shows the difference between the experimentally observed charge density distribution and the distribution calculated using the local density approximation for a non-magnetic state.

tions of 3*d* states as ''rigid'' objects where the Hubbard correction shifts the filled and unoccupied states in the opposite directions along the energy axis.[24,30] In the GGA approximation the shape of wave functions and the population of the 3*d* states depends on the local density and its gradient in the interior area of nickel ions. The LSDA+U approximation relies to a larger extent on the model assumptions and on the choice of tight-binding orbitals used for treating electron correlations in a partly filled 3*d* shell. The GGA approximation uses the one-electron orbitals as auxiliary entities required in a calculation of total density $\rho(\mathbf{r})$, which is the quantity observed experimentally using high-energy electron diffraction.

Figure 5 also shows a low resolution difference map between the experimentally observed and the GGA charge-density distribution estimated using seventy six low-order experimentally measured structure factors listed in Table I (this includes transpositions and mirror reflections). The comparison between the experimental and calculated distributions confirms the trends revealed by the GGA and LSDA+U analysis showing that correlation effects are responsible for the suppression of covalent bonding between the metal and oxygen sublattices (this effect manifests itself in the reduction of the charge density in the areas between the oxygen and nickel ions, see also Fig. 6). This agrees with the analysis of a similar effect discovered in Ref. 35 for uranium dioxide. The charge density in a unit cell of *real* NiO is more concentrated around atomic nuclei and it also shows tendency towards increasing in the region between ions of the same type. Qualitatively, this may be interpreted as an indication that Ni *d* orbitals in fact have the shape that is different from that predicted by either the GGA or the LSDA+U calculations.

There are several reasons responsible for the observed disagreement between *ab initio* calculations described above, and experimental measurements. For example, the LSDA+U approximation is based on the mean-field treatment of correlation effects.[10] There may be other, more fundamental, reason leading to the disagreement between the calculated and experimentally observed charge-density distributions. For example, one idea behind the development of more accurate approaches to the treatment of electron correlations in transition-metal compounds consists in that the new approaches are intended to be used for evaluating the parameters entering tight-binding *many-body* models of electron-electron interactions. These tight-binding models are always based on a particular choice of orbitals associated with each of the ions in the solid. Our results show that the accuracy of the assumption that the charge density may be decomposed into contributions associated with individual ions, is limited,

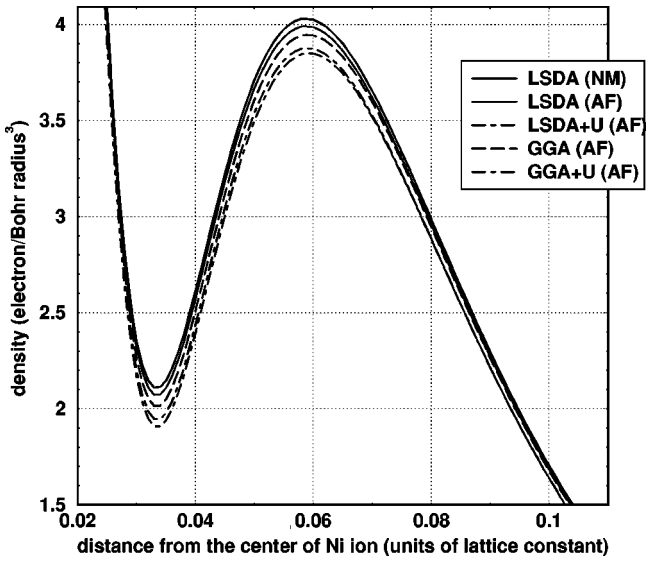

FIG. 6. Profiles of charge density along the direction of Ni-O bond calculated using the five *ab initio* approximations described in the text. Correlation effects in the 3*d* shell of Ni ions are seen to reduce the spin-dependent occupancy of e_g states that give the dominant contribution to the distribution of charge density in the direction of O-Ni bond.

and this conclusion agrees with the analysis performed in Ref. 13. To describe correlation effects in oxides where covalency as well as correlation effects play a significant part, it may be necessary to take into account changes in *both* the shape *and* occupation of localized electronic orbitals. A second quantized many-body model describing intersite hopping and on-site Coulomb interaction between electrons may prove to be sufficient for accounting for the positions of the main peaks in the spectrum of excited states of an oxide. At the same time even the exact solution of the model may not be capable of giving a sufficiently accurate description to the the ground-state properties of the system such as the distribution of the charge density in a crystal unit cell. The approach developed in this paper can also now be used to test the accuracy of several other *ab initio* methods that we did not consider above, for example, the self-interaction correction[9] or the first-principles Hartree-Fock approximation.[36]

In summary, by combining a recently developed high-accuracy electron diffraction technique with *ab initio* calculations, we investigated how electron correlations in the Ni $3d$ shell influence the distribution of charge density in the unit cell of NiO. By comparing the experimentally measured values of structure factors with values calculated using several different *ab initio* approaches we found that the structure factors evaluated using the generalized gradient approximation and the LSDA+U approach agree best with the available experimental information. The experimental data show that the degree of covalent bonding in NiO is smaller than that predicted by theoretical calculations.

We would like to thank O. K. Andersen, A. P. Sutton, and S. D. Kenny for many stimulating discussions. S. L. Dudarev acknowledges financial support from Deutscher Akademischer Austauschdienst during his visit to Max-Planck-Institut für Festkörperforschung, Stuttgart. The experimental measurements carried out at ASU HREM center were supported by NSF Grant No. DMR 9412146. Calculations were performed in the Materials Modelling Laboratory of the Department of Materials at the University of Oxford, UK using computer facilities provided by BNFL and by the EPSRC JREI grant GR/M34454. We also thank the Royal Society and the National Science Foundation of China for financial support.

*Also at: Department of Materials, University of Oxford, Parks Road, Oxford OX1 3PH, United Kingdom. Permanent address: UKAEA Fusion, D3 Culham Science Center, Abingdon, Oxfordshire OX14 3DB, United Kingdom. Electronic address: sergei.dudarev@ukaea.org.uk

†Also at: Beijing Laboratory of Electron Microscopy, Center for Condensed Matter Physics and Institute of Physics, Chinese Academy of Sciences, P.O. Box 2724, Beijing 100080, China.

[1] See, e.g., J. W. Christian, *The Theory of Transformations in Metals and Alloys*, 2nd edition (Pergamon Press, Oxford, 1975), Pt. 1. On page 1 of this monograph we read: '' . . . Although much work has been devoted to finding suitable methods of calculation, the results obtained are not encouraging, and it is not usually possible to predict the relative stabilities of different crystal structures . . . .''

[2] P. Hohenberg and W. Kohn, Phys. Rev. **136**, B864 (1964).

[3] J. M. Zuo, P. Blaha, and K. Schwartz, J. Phys. C **9**, 7541 (1997).

[4] W. Kohn and L. J. Sham, Phys. Rev. A **140**, A1133 (1965).

[5] P. Fulde, *Electron Correlations in Molecules and Solids*, 2nd ed. (Springer-Verlag, Berlin, 1995).

[6] K. Terakura, T. Oguchi, A. R. Williams, and J. Kübler, Phys. Rev. B **30**, 4734 (1984).

[7] J. Kübler and A. R. Williams, J. Magn. Magn. Mater. **54-57**, 603 (1986).

[8] M. R. Norman, Phys. Rev. Lett. **64**, 1162 (1990).

[9] A. Svane and O. Gunnarsson, Phys. Rev. Lett. **65**, 1148 (1990); Z. Szotek, W. M. Temmerman, and H. Winter, Phys. Rev. B **47**, 4029 (1993).

[10] V. I. Anisimov, Z. Zaanen, and O. K. Andersen, Phys. Rev. B **44**, 943 (1991).

[11] A. I. Liechtenstein, V. I. Anisimov, and J. Zaanen, Phys. Rev. B **52**, R5467 (1995).

[12] S. Y. Ezhov, V. I. Anisimov, H. F. Pen, D. I. Khomskii, and G. A. Sawatzky, Europhys. Lett. **44**, 491 (1998).

[13] W. P. Pickett, S. C. Erwin, and E. C. Ethridge, Phys. Rev. B **58**, 1201 (1998).

[14] J. M. Zuo, J. C. H. Spence, and M. O'Keeffe, Phys. Rev. Lett. **61**, 353 (1988).

[15] J. M. Zuo, Mater. Trans., JIM **39**, 938 (1998); J. C. H. Spence, Acta Crystallogr., Sect. A: Found. Crystallogr. **49**, 231 (1993).

[16] J. M. Zuo, M. O'Keeffe, P. Rez, and J. C. H. Spence, Phys. Rev. Lett. **78**, 4777 (1997).

[17] O. K. Andersen, Phys. Rev. B **12**, 3060 (1975).

[18] S. Y. Savrasov and D. Y. Savrasov, Phys. Rev. B **46**, 12 181 (1992); Y. Savrasov, *ibid.* **54**, 16 470 (1996).

[19] H. P. Rooksby, Acta Crystallogr. **1**, 226 (1948).

[20] V. Massarotti, D. Capsoni, V. Berbenni, R. Riccardi, A. Marini, and E. Antolini, Z. Naturforsch. A: Phys Sci **A46**, 503 (1991).

[21] J. M. Zuo, M. Kim, M. O'Keeffe, and J. C. H. Spence, Nature (London) **401**, 49 (1999).

[22] B. H. Brandow, Adv. Phys. **26**, 7345 (1977).

[23] S. Hüfner, Adv. Phys. **43**, 183 (1994).

[24] V. I. Anisimov, I. V. Solovyev, M. A. Korotin, M. T. Czyzyk, and G. A. Sawatzky, Phys. Rev. B **48**, 16 929 (1993).

[25] P. B. Hirsch, A. Howie, R. Nicholson, D. W. Pashley, and M. J. Whelan, *Electron Microscopy of Thin Crystals* (Krieger, Malabar, FL, 1977), p. 208.

[26] D. J. Eaglesham, E. P. Kvam, and C. J. Humphreys, in *EUREM'88*, Institute of Physics Conference Series No. 93 (IOP, Bristol, 1989), p. 33.

[27] J. M. Zuo, M. Kim, and R. Holmestad, J. Electron Microsc. **47**, 121 (1998).

[28] V. L. Moruzzi, J. F. Janak, and A. R. Williams, *Calculated Electronic Properties of Metals* (Pergamon, New York, 1978).

[29] J. P. Perdew, K. Burke, and M. Ernzerhof, Phys. Rev. Lett. **77**, 3865 (1996).

[30] S. L. Dudarev, G. A. Botton, S. Y. Savrasov, C. J. Humphreys, and A. P. Sutton, Phys. Rev. B **57**, 1505 (1998).

[31] O. Tjernberg, S. Söderholm, G. Chiaia, R. Girard, U. O. Karlsson, H. Nylen, and I. Lindau, Phys. Rev. B **54**, 10 245 (1996).

[32] A. Woods, W. Cochran, and B. Brockouse, Phys. Rev. **131**, 1025 (1960).

[33] H. Bilz and W. Kress, *Phonon Dispersion Relations in Insulators*,

Springer Series in Solid State Sciences Vol. 10 (Springer, Berlin, 1979), p. 57.
[34] H. X. Gao, L.-M. Peng, and J.M. Zuo, Acta Crystallogr., Sect. A: Found. Crystallogr. **55**, 1014 (1999).
[35] S. L. Dudarev, D. Nguyen Manh, and A. P. Sutton, Philos. Mag. B **75**, 613 (1997).
[36] M. D. Towler, N. L. Allan, N. M. Harrison, V. R. Saunders, W. C. Mackrodt, and E. Apra, Phys. Rev. B **50**, 5041 (1994).